Contemporary Mathematics
https://ojs.wiserpub.com/index.php/CM/

Research Article

Optical Solitons with Dispersive Concatenation Model Having Multiplicative White Noise by F-Expansion Approach

Yakup Yildirim[1,2*], Anjan Biswas[3,4,5,6]

[1] Department of Computer Engineering, Biruni University, Istanbul, 34010, Turkey
[2] Mathematics Research Center, Near East University, 99138, Nicosia, Cyprus
[3] Department of Mathematics & Physics, Grambling State University, Grambling, LA, 71245-2715, USA
[4] Department of Physics and Electronics, Khazar University, Baku, AZ-1096, Azerbaijan
[5] Department of Applied Sciences, Cross-Border Faculty of Humanities, Economics and Engineering, Dunarea de Jos University of Galati, 111 Domneasca Street, Galati, 800201, Romania
[6] Department of Mathematics and Applied Mathematics, Sefako Makgatho Health Sciences University, Medunsa, 0204, South Africa
E-mail: yyildirim@biruni.edu.tr

Received: 9 April 2025; **Revised:** 11 August 2025; **Accepted:** 14 August 2025

Abstract: The present paper offers a systematic study of the dispersive concatenation model, with special emphasis on the Kerr law nonlinearity that governs the optical interactions of photons in optical fibers. The model is studied in the environment of multiplicative white noise via the use of Itô Calculus, a stochastic method that significantly impacts the system's dynamics. To deal with the resulting complexities generated both in the form of the noise and the nonlinear dispersion, the F-expansion method is used to find the solutions of the governing equations. The strong mathematical background enables the successful identification of a wide range of optical soliton solutions, while special emphasis is given to their stability and their conditions of propagation in such environments.

Keywords: F-expansion, dispersion, white noise, solitons, concatenation

MSC: 78A60, 81V80

1. Introduction

The concatenation model, presented in 2014, is another important nonlinear evolution equation in the optical physics domain. It was synthesized as an integration of three already known systems, namely the Nonlinear Schrödinger Equation (NLSE), the Lakshmanan-Porsezian-Daniel (LPD) model, and the Sasa-Satsuma equation. The composite model, in essence, does capture basic nonlinear and dispersive properties that govern the optical fiber's pulse propagation. A later extension of the model, the so-called dispersive concatenation model, improved the system further through the emphasis of the higher-order dispersion through the integration of the Schrödinger-Hirota Equation (SHE), the LPD model, and the fifth-order NLSE [1, 2].

These models, since their introduction, have been of significant interest, particularly concerning exact optical soliton solutions and the corresponding conservation laws. Utilizing methods such as the multipliers approach, researchers have

DOI: https://doi.org/10.37256/cm.6520256955

studied conserved quantities such as energy and momentum, thus expanding the awareness of the dynamics of the soliton in the context of various physical phenomena.

A significant amount of research has examined various versions of the concatenation model, including those with and without Self-Phase Modulation (SPM), whereas Spatio-Temporal Dispersion (STD) and Chromatic Dispersion (CD) are also considered. These factors are critical in the correct simulation of long-distance pulse evolution and addressing problems such as the constraint of bandwidth in optical communications. Stable soliton solutions have been realized in scenarios involving both Kerr and power-law SPM, and in the absence of SPM, evidencing the robustness of the solitons in a wide range of nonlinear conditions. In the various analytical approaches, the Laplace-Adomian decomposition method has proved useful in the estimation of soliton solutions and examining their dynamics in complicated environments.

Building on this foundation, the present study explores the dispersive concatenation model under the influence of Multiplicative White Noise (MWN). The stochastic nature of MWN is modeled using Itô calculus, providing a rigorous framework for accounting for environmental randomness. This approach reflects the practical reality of optical systems, where fluctuations due to quantum, thermal, or external factors cannot be ignored.

To derive soliton solutions within this stochastic setting, we apply the F-expansion method, a robust analytical technique that expresses solutions in terms of Jacobi elliptic functions. In the limiting case (modulus approaching unity), these solutions reduce to classical hyperbolic solitons. The results reveal a broad spectrum of soliton profiles with varying stability characteristics, presented in detail in the following sections.

The novelty of this study lies in applying the dispersive concatenation model under Kerr-type SPM and stochastic perturbations, a combination that has received limited attention in the literature. The use of the F-expansion method in this context enables the construction of diverse soliton families and offers deeper insight into soliton dynamics in noisy environments.

Physically, the findings illustrate how solitons can persist and evolve under realistic, noise-affected conditions. The interaction between dispersion and stochasticity is particularly relevant for designing resilient optical communication systems, where maintaining signal shape and integrity is essential. The results offer theoretical guidance for improving long-distance, high-capacity data transmission in fiber networks.

Thus, this work advances both the modeling framework and solution methodology for stochastic nonlinear optics. It lays the groundwork for further exploration of soliton behavior in complex, noise-dominated media and points toward new directions in optical system design and photonic device engineering.

1.1 *Governing model*

In this study, we introduce a novel dispersive concatenation model that incorporates the Kerr law of SPM and accounts for MWN effects. The governing equation is formulated within the framework of Itô calculus, which is widely used to handle stochastic differential equations involving random perturbations. The model is given by [3]:

$$
\begin{aligned}
& iq_t + aq_{xx} + b|q|^2 q - i\delta_1 \left[\sigma_1 q_{xxx} + \sigma_2 |q|^2 q_x\right] + \sigma q W_t(t) \\
& + \delta_2 \left[\sigma_3 q_{xxxx} + \sigma_4 |q|^2 q_{xx} + \sigma_5 |q|^4 q + \sigma_6 |q_x|^2 q + \sigma_7 q_x^2 q^* + \sigma_8 q_{xx}^* q^2\right] \qquad (1) \\
& - i\delta_3 \left[\sigma_9 q_{xxxxx} + \sigma_{10} |q|^2 q_{xxx} + \sigma_{11} |q|^4 q_x + \sigma_{12} q q_x q_{xx}^* + \sigma_{13} q^* q_x q_{xx} + \sigma_{14} q q_x^* q_{xx} + \sigma_{15} q_x^2 q_x^*\right] = 0.
\end{aligned}
$$

Here, $q(x,\, t)$ represents the complex optical field envelope, with x and t denoting the spatial and temporal coordinates, respectively. The coefficients a and b model the CD and the Kerr nonlinearity, forming the basis of the NLSE. Higher-order effects are included via the parameters $\delta_1,\ \delta_2,\ \delta_3$, corresponding to third-order, fourth-order, and fifth-order nonlinear terms.

The third-order contribution δ_1 introduces q_{xxx} and a nonlinear term $|q|^2 q_x$, reflecting third-order dispersion and nonlinear dispersive effects. The fourth-order terms (δ_2) bring in the terms of q_{xxxx}, $|q|^2 q_{xx}$, and $|q|^4 q$, enabling complex nonlinear interactions that go beyond the standard models. The fifth-order terms (δ_3), in turn, continue to enrich this model further through high-order dispersive and nonlinear terms, such as q_{xxxxx} and $|q|^4 q_x$, that capture the sophisticated dynamics of ultrafast pulse propagation.

The stochastic disturbance is given by the expression $\sigma q W_t(t)$, in terms of σ, the parameter that determines the characteristics of the noise intensity, and the standard Wiener process is given below

$$W(t) = \int_0^t \Lambda(\eta) dW(\eta).$$

Here, $\Lambda(\eta)$ is Gaussian white noise. This is the physical jitter inherent in the medium, including random variation in refractive index that impacts the optical pulse's dynamical evolution. These random variations in turn will change the amplitude, shape, and robustness of solitons; therefore, including them is critical for realistic modeling in practical applications, such as fiber lasers and communication systems in the presence of noise.

The combination of stochastic perturbations with deterministic nonlinear dynamics allows for an in-depth study of the motion of solitons in applicable scenarios. Utilizing the Itô approach, this research carefully covers these deliberations and lays the ground for deriving accurate analytical results in stochastic settings.

In the paragraphs that follow, we apply the F-expansion method in obtaining accurate soliton solutions and analyzing their physical consequences. The approach offers a unified platform for the study of the stability and properties of the solitons in the presence of noise in optical telecommunication systems.

2. *F*-expansion approach

The equation is given as

$$G(q, q_x, q_t, q_{xt}, q_{xx}, \ldots) = 0. \tag{2}$$

Here, $q(x, t)$ refers to the envelope of the optical field, considering the spatial parameter x in addition to the temporal parameter t. The given mathematical expression summarizes the fundamental dynamics of the system, depicting the evolution of the optical field considering different nonlinear and dispersive effects.

We introduce the transformation of the propagating wave described in the form

$$q(x, t) = U(\xi), \; \xi = k(x - vt). \tag{3}$$

Here, v is the velocity, k is the wave width, while ξ is the new variable. By substituting this transformation into equation (2), the governing equation is reduced to an Ordinary Differential Equation (ODE) of the form

$$P(U, -kvU', kU', k^2U'', \ldots) = 0. \tag{4}$$

Step 1: To obtain exact solutions to equation (4), we assume a solution representation in the form

$$U(\xi) = \sum_{i=0}^{N} B_i F^i(\xi), \tag{5}$$

where B_i are constants to be determined and $F(\xi)$ satisfies the auxiliary equation

$$F'(\xi) = \sqrt{PF^4(\xi) + QF^2(\xi) + R}. \tag{6}$$

This equation provides a framework for constructing soliton solutions using known functions.

The functional forms of $F(\xi)$ corresponding to different types of soliton solutions are obtained from equation (6) and summarized as follows:

$$\begin{cases} F(\xi) = \mathrm{sn}(\xi) = \tanh(\xi), \; P = m^2, \; Q = -(1+m^2), \; R = 1, \; m \to 1^-, \\ F(\xi) = \mathrm{ns}(\xi) = \coth(\xi), \; P = 1, \; Q = -(1+m^2), \; R = m^2, \; m \to 1^-, \\ F(\xi) = \mathrm{cn}(\xi) = \mathrm{sech}(\xi), \; P = -m^2, \; Q = 2m^2 - 1, \; R = 1 - m^2, \; m \to 1^-, \\ F(\xi) = \mathrm{ds}(\xi) = \mathrm{csch}(\xi), \; P = 1, \; Q = 2m^2 - 1, \; R = -m^2\left(1 - m^2\right), \; m \to 1^-, \\ F(\xi) = \mathrm{ns}(\xi) \pm \mathrm{ds}(\xi) = \coth(\xi) \pm \mathrm{csch}(\xi), \; P = \dfrac{1}{4}, \; Q = \dfrac{m^2 - 2}{2}, \; R = \dfrac{m^2}{4}, \; m \to 1^-, \\ F(\xi) = \mathrm{sn}(\xi) \pm i\mathrm{cn}(\xi) = \tanh(\xi) \pm i\mathrm{sech}(\xi), \; P = \dfrac{m^2}{4}, \; Q = \dfrac{m^2 - 2}{2}, \; R = \dfrac{m^2}{4}, \; m \to 1^-, \\ F(\xi) = \dfrac{\mathrm{sn}(\xi)}{1 \pm \mathrm{dn}(\xi)} = \dfrac{\tanh(\xi)}{1 \pm \mathrm{sech}}, \; P = \dfrac{m^2}{4}, \; Q = \dfrac{m^2 - 2}{2}, \; R = \dfrac{m^2}{4}, \; m \to 1^-. \end{cases} \tag{7}$$

Here, sn(ξ), cn(ξ), dn(ξ), ns(ξ), and ds(ξ) denote Jacobi elliptic functions associated with the modulus $0 < m < 1$. In the limit $m \to 1^-$, these functions reduce to hyperbolic functions, describing bright, dark, and singular solitons. The constants B_i are determined based on the balancing principle applied to equation (4).

Step 2: Substituting expressions (5) and (6) into equation (4) results in an algebraic system of equations. Solving this system allows for the determination of the unknown constants, including B_i, ensuring that the solutions satisfy the original governing equation. These results provide an extensive classification of optical solitons, including bright solitons, dark solitons, singular solitons, and complex-valued solutions, revealing the rich nonlinear wave dynamics governed by equation (2).

3. Optical solitons

Equation (1) governs the optical field envelope, which is expressed as

$$q(x,\ t) = U(\xi)e^{i\phi(x,\ t)}, \tag{8}$$

where the variable transformation

$$\xi = k(x - vt), \tag{9}$$

is introduced to represent the wave profile in a moving frame with velocity v. The corresponding phase function is given by

$$\phi(x,\ t) = -\kappa x + \omega t + \sigma W(t) - \sigma^2 t + \theta_0. \tag{10}$$

In this formulation, ω denotes the wave number, κ represents the soliton frequency, and θ_0 is an arbitrary phase constant. The parameter σ accounts for the noise coefficient, while v represents the velocity of the soliton. The term $W(t)$ corresponds to a Wiener process, modeling the influence of MWN in the system.

To derive the governing equations for the amplitude $U(\xi)$ and the phase function $\phi(x,\ t)$, equation (8) is substituted into equation (1). By separately equating the real and imaginary components, one obtains the following coupled equations:

$$\begin{aligned}
&k^2\left(10\sigma_9\kappa^3\delta_3 - 6\sigma_3\kappa^2\delta_2 - 3\sigma_1\kappa\delta_1 + a\right)U'' + k^4\left(\sigma_3\delta_2 - 5\sigma_9\kappa\delta_3\right)U^{(4)} \\
&+ \left(\kappa^4\left(\sigma_3\delta_2 - \sigma_9\kappa\delta_3\right) + \sigma_1\kappa^3\delta_1 - a\kappa^2 + \left(\sigma^2 - \omega\right)\right)U + \left(\sigma_5\delta_2 - \sigma_{11}\kappa\delta_3\right)U^5 \\
&+ \left(\kappa^2\left(\left(\sigma_{10} + \sigma_{12} + \sigma_{13} - \sigma_{14} - \sigma_{15}\right)\kappa\delta_3 - \left(\sigma_4 - \sigma_6 + \sigma_7 + \sigma_8\right)\delta_2\right) - \sigma_2\kappa\delta_1 + b\right)U^3 \\
&+ k^2\left(\left(\sigma_4 + \sigma_8\right)\delta_2 - \left(3\sigma_{10} + \sigma_{12} + \sigma_{13} - \sigma_{14}\right)\kappa\delta_3\right)U^2U'' \\
&+ k^2\left(\left(2\sigma_{12} - 2\left(\sigma_{13} + \sigma_{14}\right) - \sigma_{15}\right)\kappa\delta_3 + \left(\sigma_6 + \sigma_7\right)\delta_2\right)UU'^2 = 0,
\end{aligned} \tag{11}$$

and

$$\begin{aligned}
&k\left(-5\sigma_9\kappa^4\delta_3 + 4\sigma_3\kappa^3\delta_2 + 3\sigma_1\kappa^2\delta_1 - 2a\kappa - v\right)U' \\
&- \sigma_9\delta_3k^5U^{(5)} - k^3\left(2\kappa\left(2\sigma_3\delta_2 - 5\sigma_9\kappa\delta_3\right) + \sigma_1\delta_1\right)U^{(3)} - \sigma_{11}k\delta_3U^4U' \\
&- \sigma_{10}\delta_3k^3U^2U^{(3)} - \sigma_{15}\delta_3k^3U'^3 - \left(\sigma_{12} + \sigma_{13} + \sigma_{14}\right)\delta_3k^3UU'U'' \\
&- k\left(\kappa\left(\left(-3\sigma_{10} + \sigma_{12} - 3\sigma_{13} + \sigma_{14} + \sigma_{15}\right)\kappa\delta_3 + 2\left(\sigma_4 + \sigma_7 - \sigma_8\right)\delta_2\right) + \sigma_2\delta_1\right)U^2U' = 0.
\end{aligned} \tag{12}$$

From equation (12), the velocity is established:

$$v=4\sigma_3\kappa^3\delta_2+3\sigma_1\kappa^2\delta_1-2a\kappa. \tag{13}$$

Additionally, the frequency is found to be

$$\kappa=\frac{(-2\sigma_2\sigma_3+\sigma_1(\sigma_4+\sigma_7-\sigma_8))\,\delta_2}{2\sigma_1\sigma_{13}\delta_3}, \tag{14}$$

alongside parametric constraints

$$\sigma_9=\sigma_{10}=\sigma_{11}=\sigma_{15}=0, \tag{15}$$

$$\sigma_{12}+\sigma_{13}+\sigma_{14}=0, \tag{16}$$

and

$$\sigma_{13}\sigma_1^2\delta_1\delta_3+2\sigma_3\left(-2\sigma_2\sigma_3+\sigma_1(\sigma_4+\sigma_7-\sigma_8)\right)\delta_2^2=0. \tag{17}$$

Thus, Eq. (1) simplifies to

$$\begin{aligned}
&iq_t+aq_{xx}+b|q|^2q-i\delta_1\left[\sigma_1q_{xxx}+\sigma_2|q|^2q_x\right]+\sigma qW_t(t)\\
&+\delta_2\left[\sigma_3q_{xxxx}+\sigma_4|q|^2q_{xx}+\sigma_5|q|^4q+\sigma_6|q_x|^2q+\sigma_7q_x^2q^*+\sigma_8q_{xx}^*q^2\right]\\
&-i\delta_3\left[\sigma_{12}qq_xq_{xx}^*+\sigma_{13}q^*q_xq_{xx}+\sigma_{14}qq_x^*q_{xx}\right]=0,
\end{aligned} \tag{18}$$

and Eq. (11) becomes

$$\begin{aligned}
&k^2\left(-6\sigma_3\kappa^2\delta_2-3\sigma_1\kappa\delta_1+a\right)U''+k^2\left(2\sigma_{14}\kappa\delta_3+\sigma_4\delta_2+\sigma_8\delta_2\right)U^2U''\\
&+\left(\sigma_3\kappa^4\delta_2+\sigma_1\kappa^3\delta_1-a\kappa^2+\sigma^2-\omega\right)U+\sigma_3k^4\delta_2U^{(4)}\\
&+\left(-2\sigma_{14}\kappa^3\delta_3-\sigma_4\kappa^2\delta_2+\sigma_6\kappa^2\delta_2-\sigma_7\kappa^2\delta_2-\sigma_8\kappa^2\delta_2-\sigma_2\kappa\delta_1+b\right)U^3\\
&+k^2\left(-4(\sigma_{13}+\sigma_{14})\kappa\delta_3+\sigma_6\delta_2+\sigma_7\delta_2\right)UU'^2+\sigma_5\delta_2U^5=0.
\end{aligned} \tag{19}$$

Also, Equation (19) transforms into

$$k^2U^{(4)} + \lambda_6 U^2 U'' + \lambda_5 U'' + \lambda_4 U U'^2 + \lambda_3 U^5 + \lambda_2 U^3 + \lambda_1 U = 0, \tag{20}$$

with

$$\begin{cases} \lambda_3 = \dfrac{\sigma_5}{\sigma_3 k^2}, \;\; \lambda_1 = \dfrac{\sigma_3 \kappa^4 \delta_2 + \sigma_1 \kappa^3 \delta_1 - a\kappa^2 + \left(\sigma^2 - \omega\right)}{\sigma_3 k^2 \delta_2}, \\[2ex] \lambda_2 = \dfrac{b - \kappa\left(\kappa\left(2\sigma_{14}\kappa\delta_3 + \left(\sigma_4 - \sigma_6 + \sigma_7 + \sigma_8\right)\delta_2\right) + \sigma_2\delta_1\right)}{\sigma_3 k^2 \delta_2}, \\[2ex] \lambda_4 = \dfrac{\left(\sigma_6 + \sigma_7\right)\delta_2 - 4\left(\sigma_{13} + \sigma_{14}\right)\kappa\delta_3}{\sigma_3\delta_2}, \\[2ex] \lambda_5 = \dfrac{-3\kappa\left(2\sigma_3\kappa\delta_2 + \sigma_1\delta_1\right) + a}{\sigma_3\delta_2}, \\[2ex] \lambda_6 = \dfrac{2\sigma_{14}\kappa\delta_3 + \left(\sigma_4 + \sigma_8\right)\delta_2}{\sigma_3\delta_2}, \end{cases} \tag{21}$$

with $\sigma_3 \neq 0$, $k \neq 0$ and $\delta_2 \neq 0$. From the requirement that U^5 and $U^{(4)}$ are in balance within equation (20), we derive $N = 1$, yielding

$$U(\xi) = B_0 + B_1 F(\xi). \tag{22}$$

After substituting (22) and (6) into (22), the equations are derived as:

$$\begin{cases} {B_0}^5\lambda_3 + RB_0{B_1}^2\lambda_4 + {B_0}^3\lambda_2 + B_0\lambda_1 = 0, \\[2ex] 12\,PRk^2B_1 + Q{B_0}^2B_1\lambda_6 + Q^2k^2B_1 + QB_1\lambda_5 + R{B_1}^3\lambda_4 + 5\,{B_0}^4B_1\lambda_3 + 3\,{B_0}^2B_1\lambda_2 + B_1\lambda_1 = 0, \\[2ex] 10\,{B_0}^3{B_1}^2\lambda_3 + QB_0{B_1}^2\lambda_4 + 2\,QB_0{B_1}^2\lambda_6 + 3\,B_0{B_1}^2\lambda_2 = 0, \\[2ex] 10\,{B_0}^2{B_1}^3\lambda_3 + 20\,PQk^2B_1 + 2\,P{B_0}^2B_1\lambda_6 + Q{B_1}^3\lambda_4 + Q{B_1}^3\lambda_6 + {B_1}^3\lambda_2 + 2\,PB_1\lambda_5 = 0, \\[2ex] 5\,B_0{B_1}^4\lambda_3 + PB_0{B_1}^2\lambda_4 + 4\,PB_0{B_1}^2\lambda_6 = 0, \\[2ex] {B_1}^5\lambda_3 + 24\,P^2k^2B_1 + P{B_1}^3\lambda_4 + 2\,P{B_1}^3\lambda_6 = 0. \end{cases} \tag{23}$$

Through solving (23), the following expressions are revealed:

$$
\begin{cases}
k = \pm\sqrt{-\dfrac{2P\lambda_5 R\lambda_4 - Q^2\lambda_4\lambda_5 - Q^2\lambda_5\lambda_6 - Q\lambda_1\lambda_4 - Q\lambda_1\lambda_6 - Q\lambda_2\lambda_5 - \lambda_1\lambda_2}{8PQR\lambda_4 - 12PQR\lambda_6 - Q^3\lambda_4 - Q^3\lambda_6 - 12PR\lambda_2 - Q^2\lambda_2}}, \\
B_0 = 0,\ \ B_1 = \pm\sqrt{-\dfrac{-24P^2R\lambda_5 + 18PQ^2\lambda_5 + 20PQ\lambda_1}{8PQR\lambda_4 - 12PQR\lambda_6 - Q^3\lambda_4 - Q^3\lambda_6 - 12PR\lambda_2 - Q^2\lambda_2}}, \\
\lambda_3 = \dfrac{\begin{pmatrix} 12P\lambda_5 R\lambda_4 - 24PR\lambda_5\lambda_6 - 3Q^2\lambda_4\lambda_5 + 6Q^2\lambda_5\lambda_6 \\ -2Q\lambda_1\lambda_4 + 8Q\lambda_1\lambda_6 - 12Q\lambda_2\lambda_5 - 12\lambda_1\lambda_2 \end{pmatrix}\begin{pmatrix} 8PQR\lambda_4 - 12PQR\lambda_6 - Q^3\lambda_4 \\ -Q^3\lambda_6 - 12PR\lambda_2 - Q^2\lambda_2 \end{pmatrix}}{2\left(144P^2R^2{\lambda_5}^2 - 216PQ^2R{\lambda_5}^2 + 81Q^4{\lambda_5}^2 - 240PQR\lambda_1\lambda_5 + 180Q^3\lambda_1\lambda_5 + 100Q^2{\lambda_1}^2\right)}.
\end{cases}
\tag{24}
$$

Result 1:
From (7), Eq. (24) is modified to

$$
\begin{cases}
k = \pm\sqrt{-\dfrac{\lambda_1\lambda_2 - 2\lambda_1\lambda_4 - 2\lambda_1\lambda_6 - 2\lambda_2\lambda_5 + 2\lambda_5\lambda_4 + 4\lambda_5\lambda_6}{16\lambda_2 + 8\lambda_4 - 32\lambda_6}}, \\
B_0 = 0,\ B_1 = \pm\sqrt{-\dfrac{5\lambda_1 - 6\lambda_5}{2\lambda_2 + \lambda_4 - 4\lambda_6}}, \\
\lambda_3 = \dfrac{(3\lambda_1\lambda_2 - \lambda_1\lambda_4 + 4\lambda_1\lambda_6 - 6\lambda_2\lambda_5)(2\lambda_2 + \lambda_4 - 4\lambda_6)}{25{\lambda_1}^2 - 60\lambda_1\lambda_5 + 36{\lambda_5}^2}.
\end{cases}
\tag{25}
$$

Accordingly, the mathematical expressions for dark and singular solitons take the form

$$
\begin{aligned}
q(x,\ t) = \pm\sqrt{-\frac{5\lambda_1 - 6\lambda_5}{2\lambda_2 + \lambda_4 - 4\lambda_6}} \\
\times \tanh\left[\begin{array}{l} \sqrt{-\dfrac{\lambda_1\lambda_2 - 2\lambda_1\lambda_4 - 2\lambda_1\lambda_6 - 2\lambda_2\lambda_5 + 2\lambda_5\lambda_4 + 4\lambda_5\lambda_6}{16\lambda_2 + 8\lambda_4 - 32\lambda_6}} \\ \times\left(x - \left(4\sigma_3\kappa^3\delta_2 + 3\sigma_1\kappa^2\delta_1 - 2a\kappa\right)t\right) \end{array}\right] \\
\times e^{i\left(-\frac{(-2\sigma_2\sigma_3 + \sigma_1(\sigma_4 + \sigma_7 - \sigma_8))\delta_2}{2\sigma_1\sigma_{13}\delta_3}x + \omega t + \sigma W(t) - \sigma^2 t + \theta_0\right)},
\end{aligned}
\tag{26}
$$

and

$$q(x,\ t)=\pm\sqrt{-\frac{5\lambda_1-6\lambda_5}{2\lambda_2+\lambda_4-4\lambda_6}}$$

$$\times\coth\left[\sqrt{-\frac{\lambda_1\lambda_2-2\lambda_1\lambda_4-2\lambda_1\lambda_6-2\lambda_2\lambda_5+2\lambda_5\lambda_4+4\lambda_5\lambda_6}{16\lambda_2+8\lambda_4-32\lambda_6}}\times\left(x-\left(4\sigma_3\kappa^3\delta_2+3\sigma_1\kappa^2\delta_1-2a\kappa\right)t\right)\right] \tag{27}$$

$$\times e^{i\left(-\frac{(-2\sigma_2\sigma_3+\sigma_1(\sigma_4+\sigma_7-\sigma_8))\delta_2}{2\sigma_1\sigma_{13}\delta_3}x+\omega t+\sigma W(t)-\sigma^2 t+\theta_0\right)}.$$

The waveforms expressed in equations (26) and (27) are constrained by the parameters:

$$\begin{aligned}&(5\lambda_1-6\lambda_5)(2\lambda_2+\lambda_4-4\lambda_6)<0,\\&(\lambda_1\lambda_2-2\lambda_1\lambda_4-2\lambda_1\lambda_6-2\lambda_2\lambda_5+2\lambda_5\lambda_4+4\lambda_5\lambda_6)(16\lambda_2+8\lambda_4-32\lambda_6)<0.\end{aligned} \tag{28}$$

Result 2:
With (7), Eq. (24) converts into

$$\begin{cases}k=\pm\sqrt{-(\lambda_1+\lambda_5)},\ B_0=0,\ \ B_1=\pm\sqrt{-\frac{20\lambda_1+18\lambda_5}{\lambda_2+\lambda_4+\lambda_6}},\\ \lambda_3=\frac{\begin{pmatrix}12\lambda_1\lambda_2{}^2+14\lambda_1\lambda_2\lambda_4+4\lambda_1\lambda_2\lambda_6+2\lambda_1\lambda_4{}^2-6\lambda_1\lambda_4\lambda_6-8\lambda_1\lambda_6{}^2\\+12\lambda_2{}^2\lambda_5+15\lambda_2\lambda_4\lambda_5+6\lambda_2\lambda_5\lambda_6+3\lambda_4{}^2\lambda_5-3\lambda_4\lambda_5\lambda_6-6\lambda_5\lambda_6{}^2\end{pmatrix}}{2\left(100\lambda_1{}^2+180\lambda_1\lambda_5+81\lambda_5{}^2\right)}.\end{cases} \tag{29}$$

Furthermore, the solution for the bright soliton takes the form

$$\begin{aligned}q(x,\ t)&=\pm\sqrt{-\frac{20\lambda_1+18\lambda_5}{\lambda_2+\lambda_4+\lambda_6}}\times\operatorname{sech}\left[\sqrt{-(\lambda_1+\lambda_5)}\left(x-\left(4\sigma_3\kappa^3\delta_2+3\sigma_1\kappa^2\delta_1-2a\kappa\right)t\right)\right]\\&\times e^{i\left(-\frac{(-2\sigma_2\sigma_3+\sigma_1(\sigma_4+\sigma_7-\sigma_8))\delta_2}{2\sigma_1\sigma_{13}\delta_3}x+\omega t+\sigma W(t)-\sigma^2 t+\theta_0\right)}.\end{aligned} \tag{30}$$

The wave form expressed in (30) is constrained by the relations:

$$(20\lambda_1 + 18\lambda_5)(\lambda_2 + \lambda_4 + \lambda_6) < 0, \;\; \lambda_1 + \lambda_5 < 0. \tag{31}$$

Result 3:
With (7), Eq. (24) is modified to

$$\begin{cases} k = \pm\sqrt{-(\lambda_1+\lambda_5)}, \; B_0 = 0, \;\; B_1 = \pm\sqrt{\dfrac{20\lambda_1 + 18\lambda_5}{\lambda_2 + \lambda_4 + \lambda_6}}, \\ \lambda_3 = \dfrac{\begin{pmatrix} 12\lambda_1{\lambda_2}^2 + 14\lambda_1\lambda_2\lambda_4 + 4\lambda_1\lambda_2\lambda_6 + 2\lambda_1{\lambda_4}^2 - 6\lambda_1\lambda_4\lambda_6 - 8\lambda_1{\lambda_6}^2 \\ + 12{\lambda_2}^2\lambda_5 + 15\lambda_2\lambda_4\lambda_5 + 6\lambda_2\lambda_5\lambda_6 + 3{\lambda_4}^2\lambda_5 - 3\lambda_4\lambda_5\lambda_6 - 6\lambda_5{\lambda_6}^2 \end{pmatrix}}{2\left(100{\lambda_1}^2 + 180\lambda_1\lambda_5 + 81{\lambda_5}^2\right)}. \end{cases} \tag{32}$$

Accordingly, the singular soliton is represented by the solution

$$\begin{aligned} q(x, t) = &\pm\sqrt{\frac{20\lambda_1 + 18\lambda_5}{\lambda_2 + \lambda_4 + \lambda_6}} \times \operatorname{csch}\left[\sqrt{-(\lambda_1+\lambda_5)}\left(x - \left(4\sigma_3\kappa^3\delta_2 + 3\sigma_1\kappa^2\delta_1 - 2a\kappa\right)t\right)\right] \\ &\times e^{i\left(-\frac{(-2\sigma_2\sigma_3 + \sigma_1(\sigma_4 + \sigma_7 - \sigma_8))\delta_2}{2\sigma_1\sigma_{13}\delta_3}x + \omega t + \sigma W(t) - \sigma^2 t + \theta_0\right)}. \end{aligned} \tag{33}$$

Equation (33) defines the wave form, subject to the constraint relations:

$$(20\lambda_1 + 18\lambda_5)(\lambda_2 + \lambda_4 + \lambda_6) > 0, \;\; \lambda_1 + \lambda_5 < 0. \tag{34}$$

Result 4:
Utilizing (7), Eq. (24) changes to

$$\begin{cases} k = \pm\sqrt{-\dfrac{8\lambda_1\lambda_2 - 4\lambda_1\lambda_4 - 4\lambda_1\lambda_6 - 4\lambda_2\lambda_5 + \lambda_5\lambda_4 + 2\lambda_5\lambda_6}{8\lambda_2 + \lambda_4 - 4\lambda_6}}, \\ B_0 = 0, \; B_1 = \pm\sqrt{-\dfrac{20\lambda_1 - 6\lambda_5}{8\lambda_2 + \lambda_4 - 4\lambda_6}}, \\ \lambda_3 = \dfrac{(12\lambda_1\lambda_2 - \lambda_1\lambda_4 + 4\lambda_1\lambda_6 - 6\lambda_2\lambda_5)(8\lambda_2 + \lambda_4 - 4\lambda_6)}{4\left(100{\lambda_1}^2 - 60\lambda_1\lambda_5 + 9{\lambda_5}^2\right)}. \end{cases} \tag{35}$$

Accordingly, the solution that represents the straddled singular-singular soliton is

$$q(x,\, t) = \pm\sqrt{-\frac{20\lambda_1 - 6\lambda_5}{8\lambda_2 + \lambda_4 - 4\lambda_6}}$$

$$\times \left\{ \begin{array}{l} \coth\left[\begin{array}{l} \sqrt{-\dfrac{8\lambda_1\lambda_2 - 4\lambda_1\lambda_4 - 4\lambda_1\lambda_6 - 4\lambda_2\lambda_5 + \lambda_5\lambda_4 + 2\lambda_5\lambda_6}{8\lambda_2 + \lambda_4 - 4\lambda_6}} \\ \times \left(x - \left(4\sigma_3\kappa^3\delta_2 + 3\sigma_1\kappa^2\delta_1 - 2a\kappa\right)t\right) \end{array} \right] \\ \pm\,\mathrm{csch}\left[\begin{array}{l} \sqrt{-\dfrac{8\lambda_1\lambda_2 - 4\lambda_1\lambda_4 - 4\lambda_1\lambda_6 - 4\lambda_2\lambda_5 + \lambda_5\lambda_4 + 2\lambda_5\lambda_6}{8\lambda_2 + \lambda_4 - 4\lambda_6}} \\ \times \left(x - \left(4\sigma_3\kappa^3\delta_2 + 3\sigma_1\kappa^2\delta_1 - 2a\kappa\right)t\right) \end{array} \right] \end{array} \right\} \tag{36}$$

$$\times e^{i\left(-\frac{(-2\sigma_2\sigma_3 + \sigma_1(\sigma_4 + \sigma_7 - \sigma_8))\delta_2}{2\sigma_1\sigma_{13}\delta_3}x + \omega t + \sigma W(t) - \sigma^2 t + \theta_0\right)}.$$

Moreover, the complexiton solution is formulated as

$$q(x,\, t) = \pm\sqrt{-\frac{20\lambda_1 - 6\lambda_5}{8\lambda_2 + \lambda_4 - 4\lambda_6}}$$

$$\times \left\{ \begin{array}{l} \tanh\left[\begin{array}{l} \sqrt{-\dfrac{8\lambda_1\lambda_2 - 4\lambda_1\lambda_4 - 4\lambda_1\lambda_6 - 4\lambda_2\lambda_5 + \lambda_5\lambda_4 + 2\lambda_5\lambda_6}{8\lambda_2 + \lambda_4 - 4\lambda_6}} \\ \times \left(x - \left(4\sigma_3\kappa^3\delta_2 + 3\sigma_1\kappa^2\delta_1 - 2a\kappa\right)t\right) \end{array} \right] \\ \pm\, i\,\mathrm{sech}\left[\begin{array}{l} \sqrt{-\dfrac{8\lambda_1\lambda_2 - 4\lambda_1\lambda_4 - 4\lambda_1\lambda_6 - 4\lambda_2\lambda_5 + \lambda_5\lambda_4 + 2\lambda_5\lambda_6}{8\lambda_2 + \lambda_4 - 4\lambda_6}} \\ \times \left(x - \left(4\sigma_3\kappa^3\delta_2 + 3\sigma_1\kappa^2\delta_1 - 2a\kappa\right)t\right) \end{array} \right] \end{array} \right\} \tag{37}$$

$$\times e^{i\left(-\frac{(-2\sigma_2\sigma_3 + \sigma_1(\sigma_4 + \sigma_7 - \sigma_8))\delta_2}{2\sigma_1\sigma_{13}\delta_3}x + \omega t + \sigma W(t) - \sigma^2 t + \theta_0\right)}.$$

Furthermore, the dark-bright soliton takes the form

$$q(x,\, t) = \pm\sqrt{-\frac{20\lambda_1 - 6\lambda_5}{8\lambda_2 + \lambda_4 - 4\lambda_6}}$$

$$\times \left\{ \frac{\tanh\left[\sqrt{-\frac{8\lambda_1\lambda_2 - 4\lambda_1\lambda_4 - 4\lambda_1\lambda_6 - 4\lambda_2\lambda_5 + \lambda_5\lambda_4 + 2\lambda_5\lambda_6}{8\lambda_2 + \lambda_4 - 4\lambda_6}} \times \left(x - \left(4\sigma_3\kappa^3\delta_2 + 3\sigma_1\kappa^2\delta_1 - 2a\kappa\right)t\right)\right]}{1 \pm \operatorname{sech}\left[\sqrt{-\frac{8\lambda_1\lambda_2 - 4\lambda_1\lambda_4 - 4\lambda_1\lambda_6 - 4\lambda_2\lambda_5 + \lambda_5\lambda_4 + 2\lambda_5\lambda_6}{8\lambda_2 + \lambda_4 - 4\lambda_6}} \times \left(x - \left(4\sigma_3\kappa^3\delta_2 + 3\sigma_1\kappa^2\delta_1 - 2a\kappa\right)t\right)\right]} \right\} \tag{38}$$

$$\times e^{i\left(-\frac{(-2\sigma_2\sigma_3 + \sigma_1(\sigma_4 + \sigma_7 - \sigma_8))\delta_2}{2\sigma_1\sigma_{13}\delta_3}x + \omega t + \sigma W(t) - \sigma^2 t + \theta_0\right)}.$$

Equations (37)-(39) define the wave forms, constrained by the parameters:

$$\begin{aligned} &(20\lambda_1 - 6\lambda_5)(8\lambda_2 + \lambda_4 - 4\lambda_6) < 0, \\ &(8\lambda_1\lambda_2 - 4\lambda_1\lambda_4 - 4\lambda_1\lambda_6 - 4\lambda_2\lambda_5 + \lambda_5\lambda_4 + 2\lambda_5\lambda_6)(8\lambda_2 + \lambda_4 - 4\lambda_6) < 0. \end{aligned} \tag{39}$$

4. Results and discussion

This section analyzes the soliton behaviors illustrated in Figures 1-15, covering dark, bright, and hybrid dark-bright solitons under varying noise levels (σ) and time steps ($t = 2.1$ to 3.0). All simulations use a consistent parameter set to ensure comparability across cases. They are: $\theta_0 = 1$, $\omega = 1$, $\delta_2 = 1$, $\delta_3 = 1$, $\sigma_4 = 1$, $\sigma_3 = 1$, $\sigma_2 = 1$, $\sigma_1 = 1$, $\sigma_7 = 1$, $\sigma_8 = 1$, $\sigma_{13} = 1$, $\delta_1 = 1$, $a = 1$, $k = 1$, $\sigma_6 = 1$, $\sigma_{14} = 1$, and $b = 1$.

Based on solution (26), the evolution of dark solitons is presented with increasing MWN levels. Figure 1 shows the soliton profile without noise, highlighting its typical intensity dip through 3D, contour, and 2D plots. As σ increases from 2 to 5 (Figures 2-5), the soliton undergoes gradual deformation: its central dip broadens, amplitude decreases, and phase coherence weakens. These effects reflect the soliton's sensitivity to noise, particularly in its spatial structure.

Described by solution (30), bright solitons display a pronounced intensity peak in the noise-free case (Figure 6). With increasing noise levels (Figures 7-10), the peak becomes less localized and loses height, while the surrounding region broadens. The 2D and contour plots illustrate these changes clearly, indicating a more pronounced degradation compared to dark solitons.

Solution (39) governs the hybrid structures combining both dark dips and bright peaks. Without noise (Figure 11), these solitons maintain distinct features of both types. However, with rising σ (Figures 12-15), the contrast between dark and bright regions diminishes. The bright peak spreads, and the dark trough becomes shallower, leading to a more uniform, less defined structure.

Across all soliton types, MWN disrupts localization and coherence. Dark solitons are relatively robust but eventually lose contrast. Bright solitons are more susceptible, showing early and significant deformations. Dark-bright solitons exhibit combined instability effects. These results confirm that MWN plays a critical role in soliton stability, with implications for real-world optical systems where noise cannot be neglected.

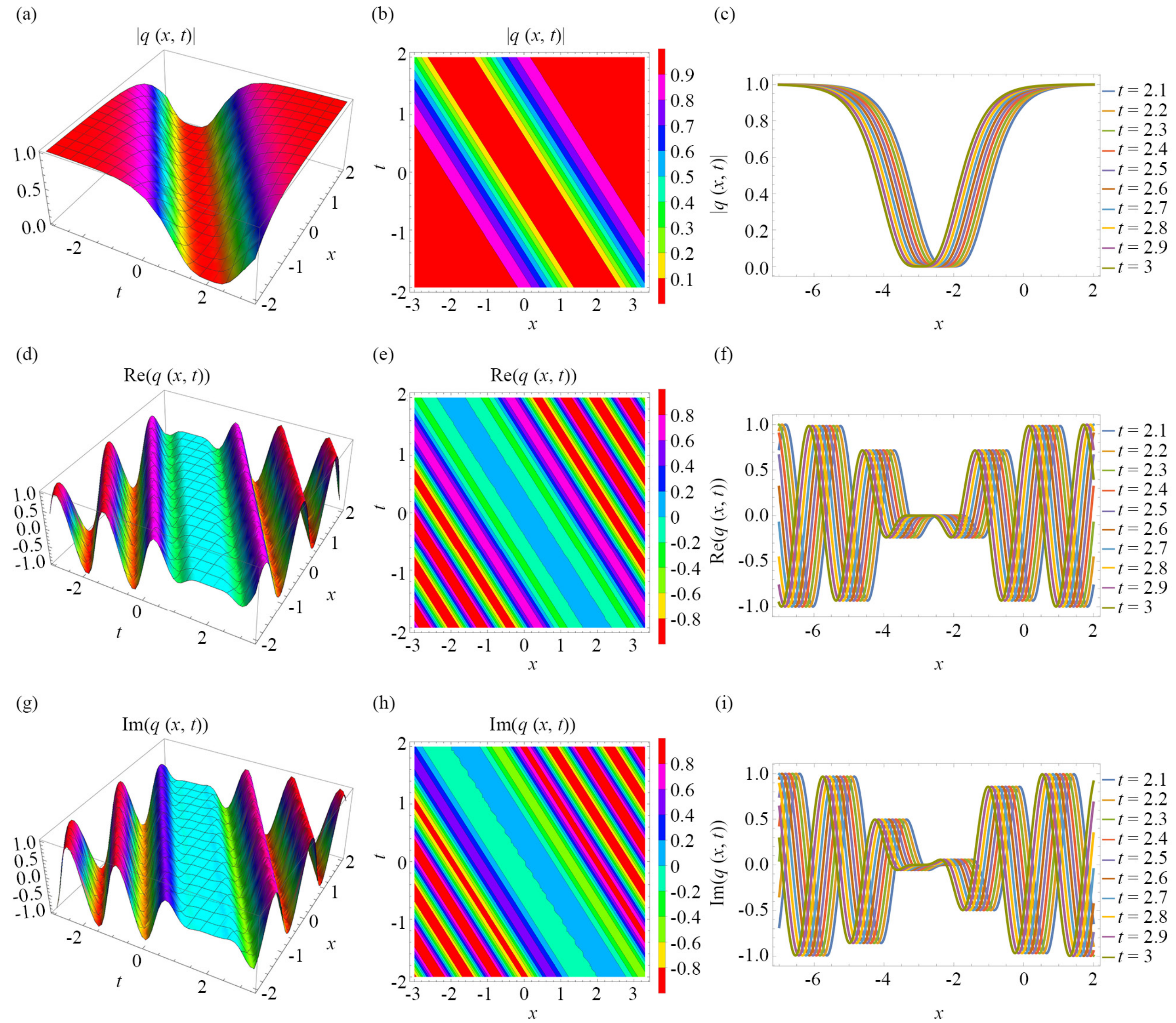

Figure 1. A dark soliton given $\sigma = 0$

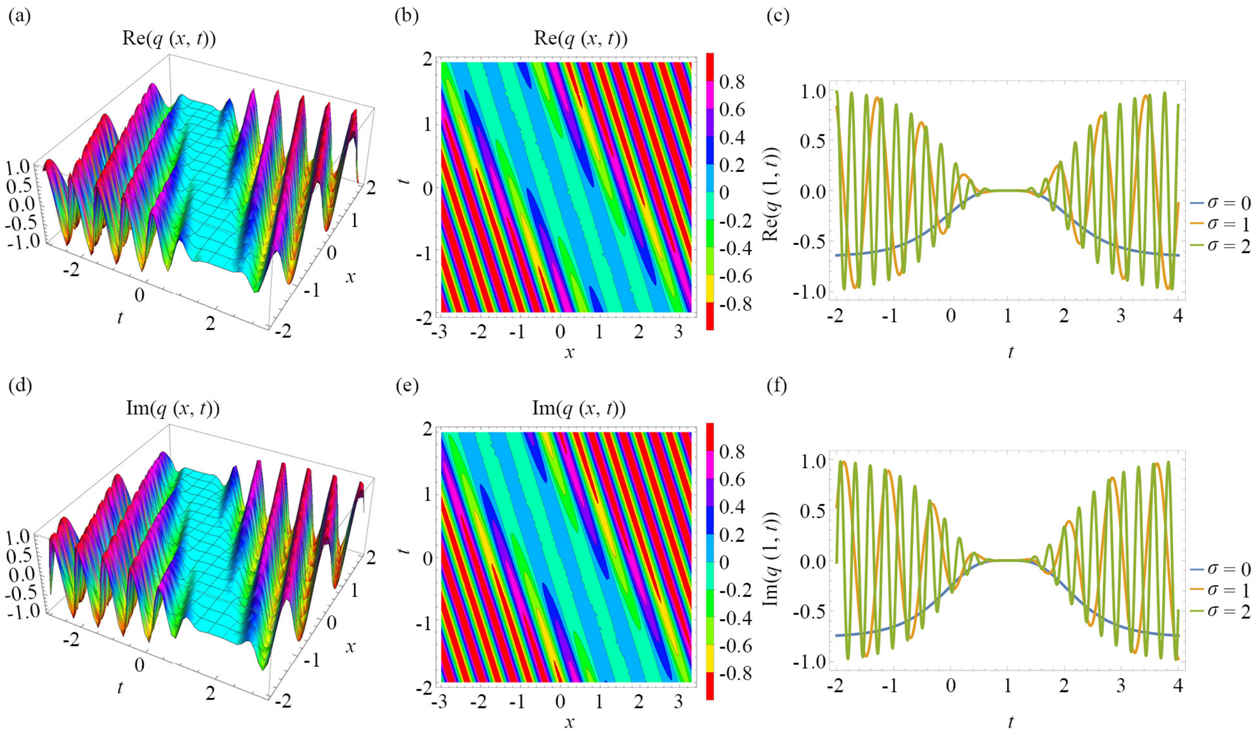

Figure 2. A dark soliton given $\sigma = 2$

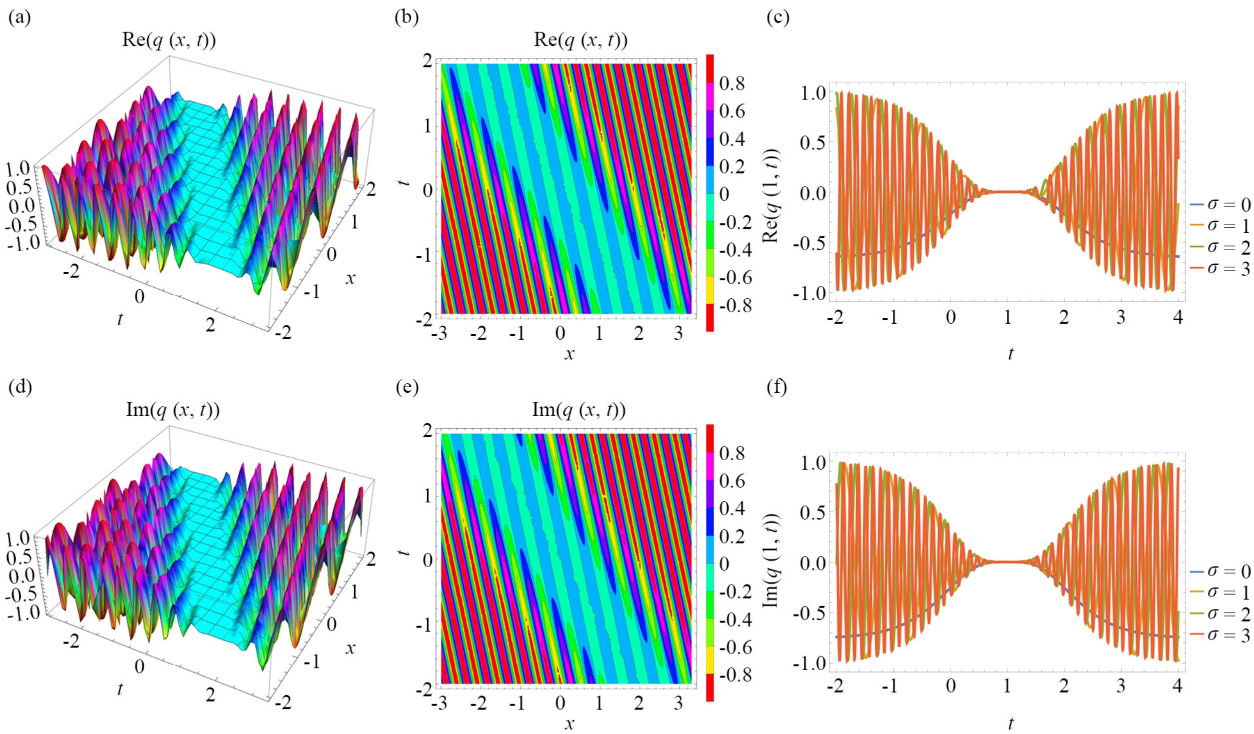

Figure 3. A dark soliton given $\sigma = 3$

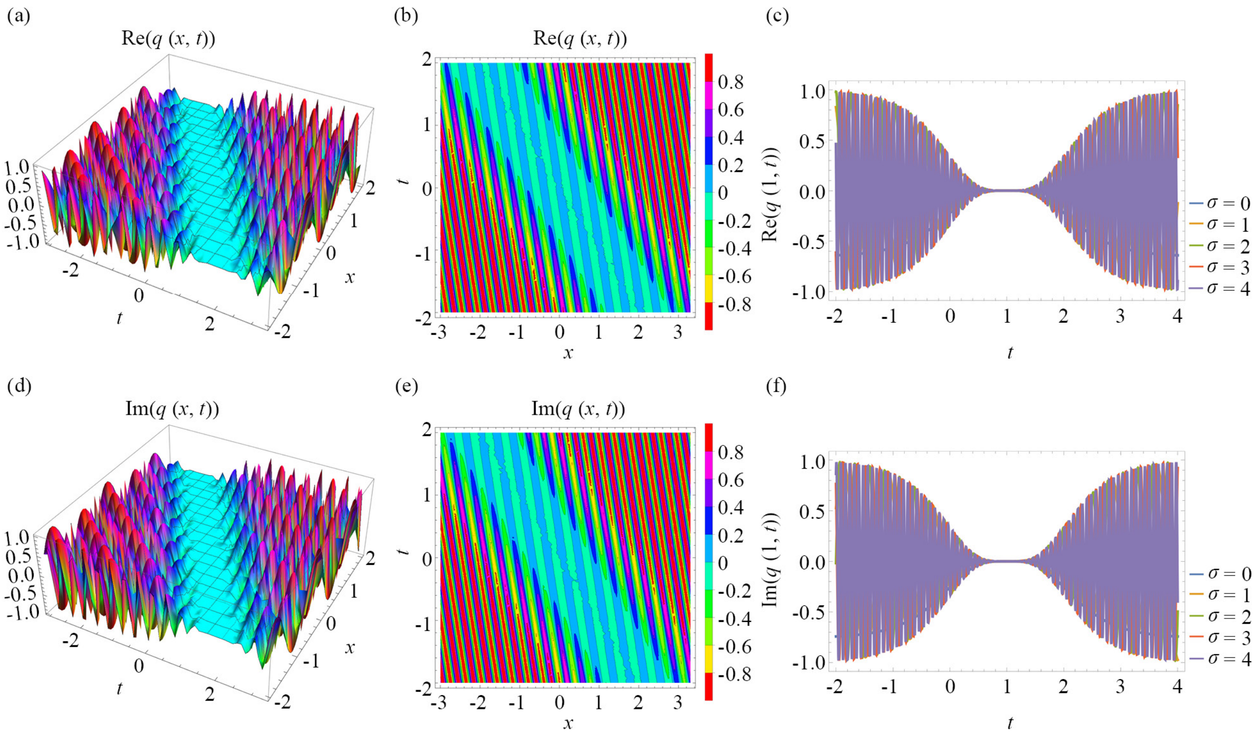

Figure 4. A dark soliton given $\sigma = 4$

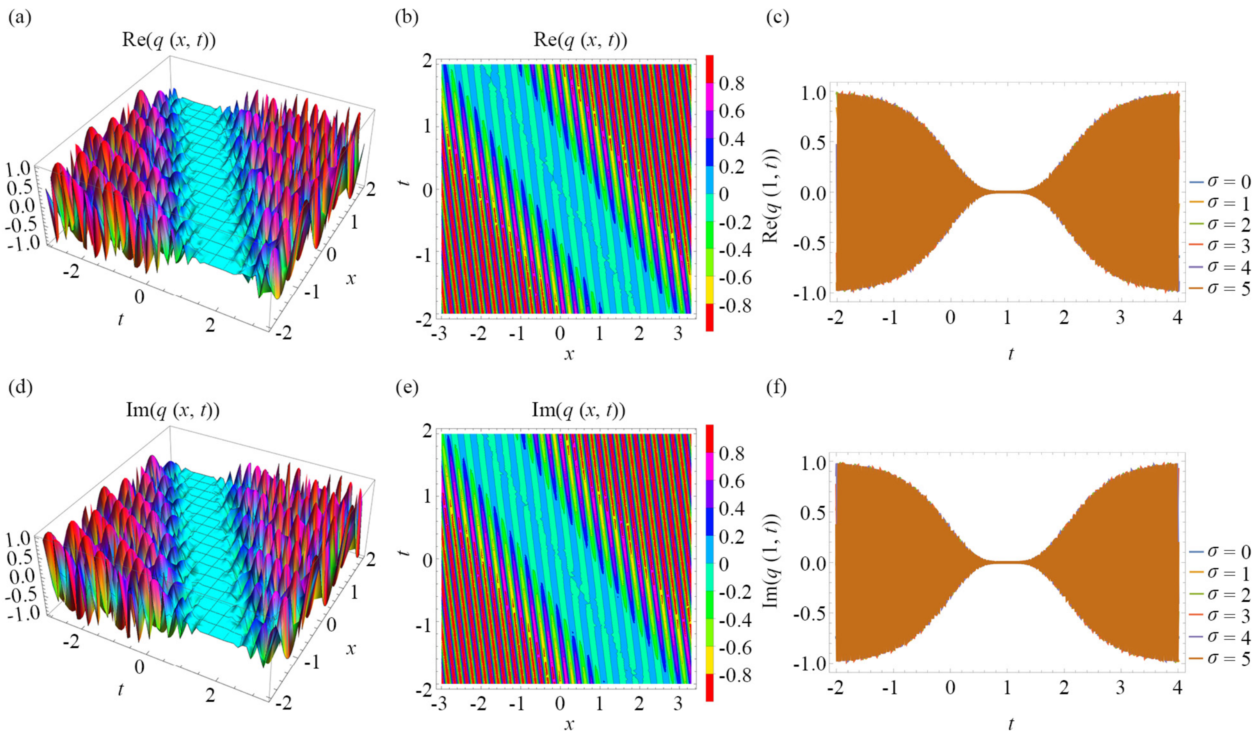

Figure 5. A dark soliton given $\sigma = 5$

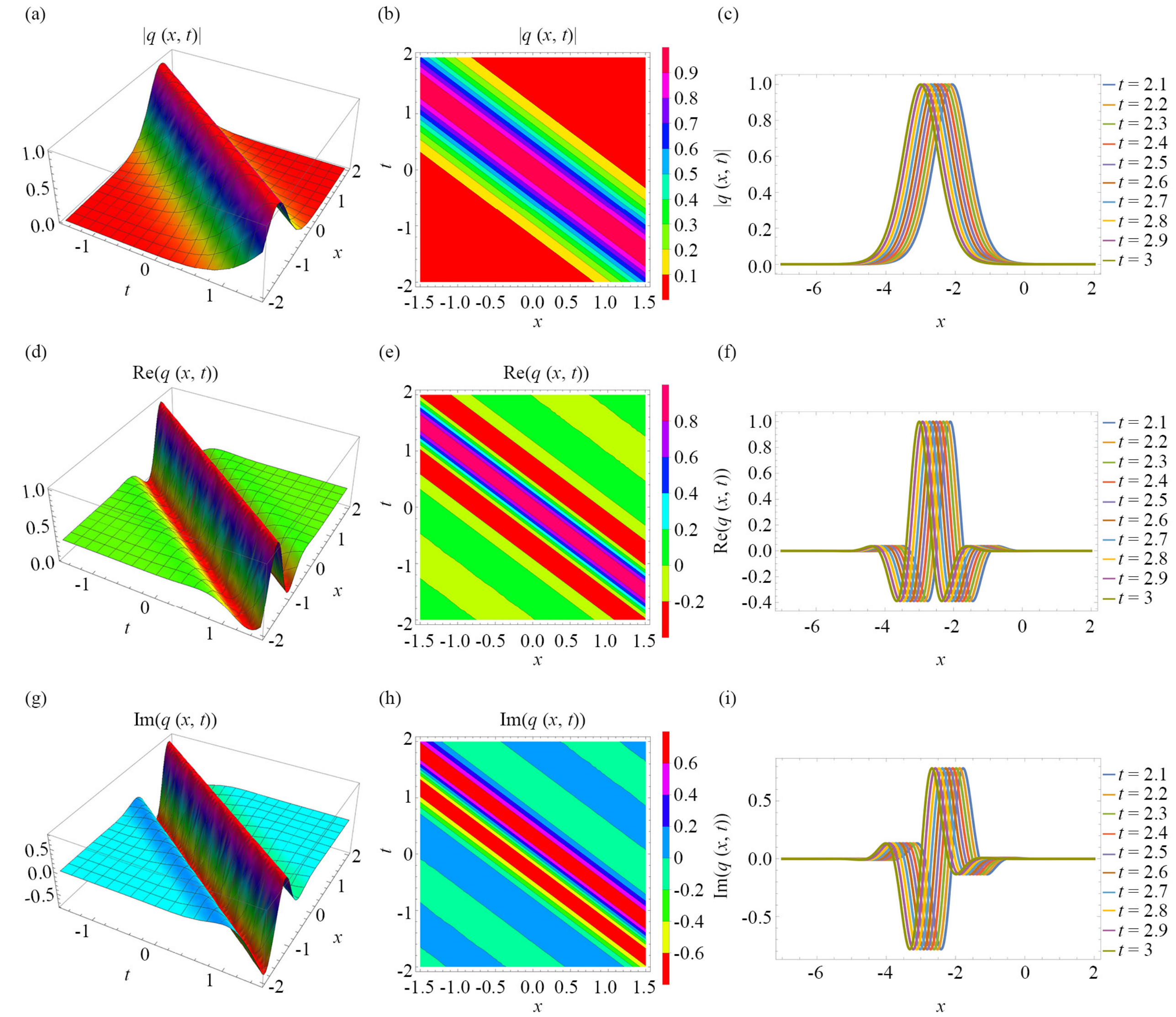

Figure 6. A bright soliton given $\sigma = 0$

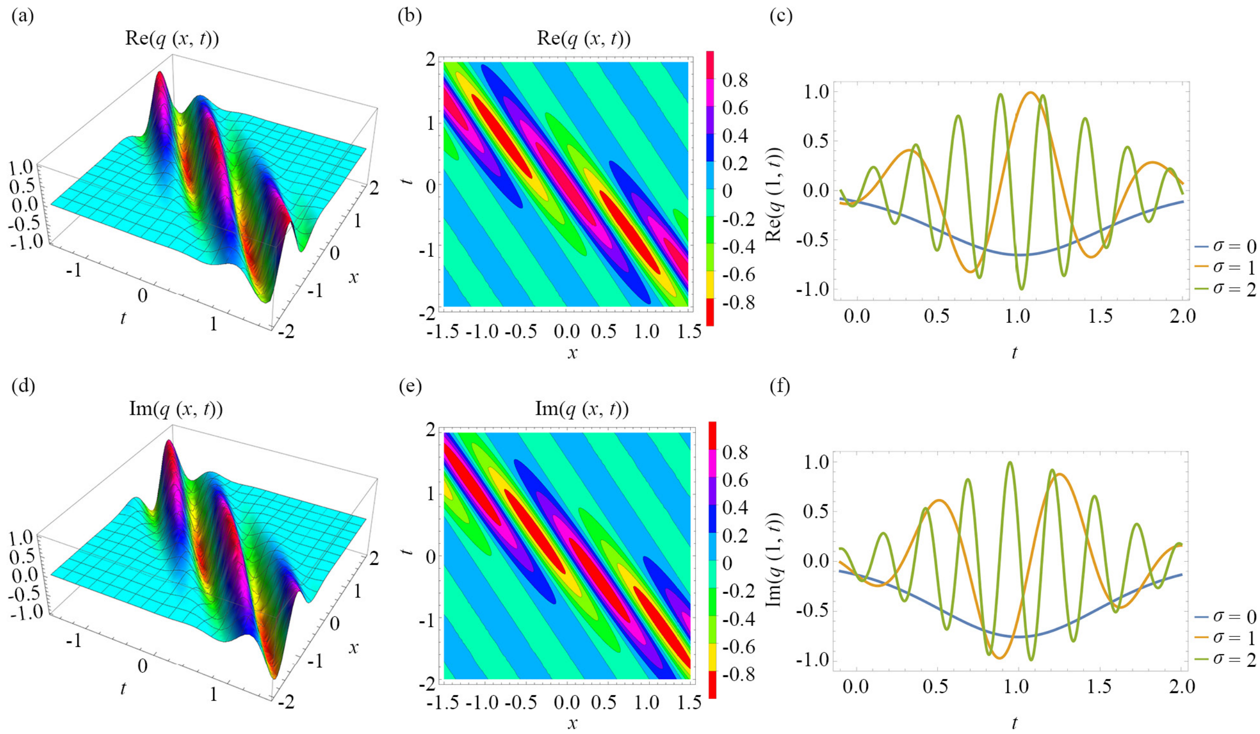

Figure 7. A bright soliton given $\sigma = 2$

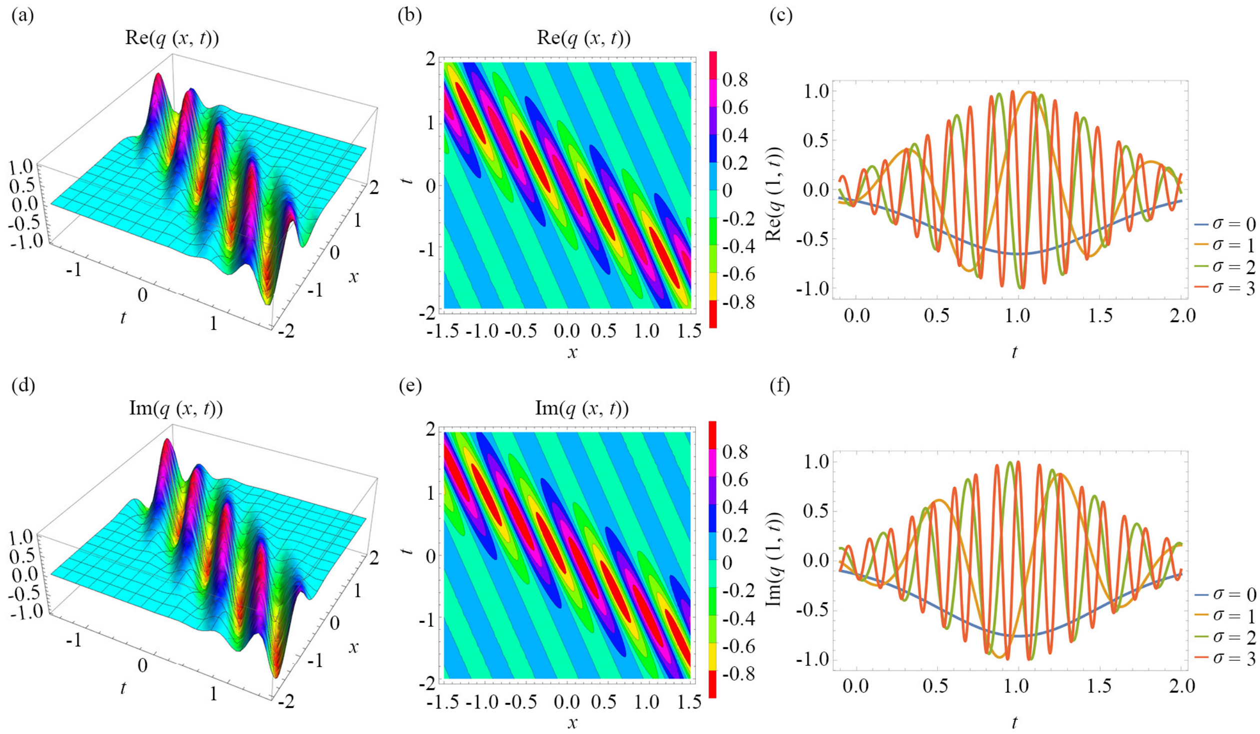

Figure 8. A bright soliton given $\sigma = 3$

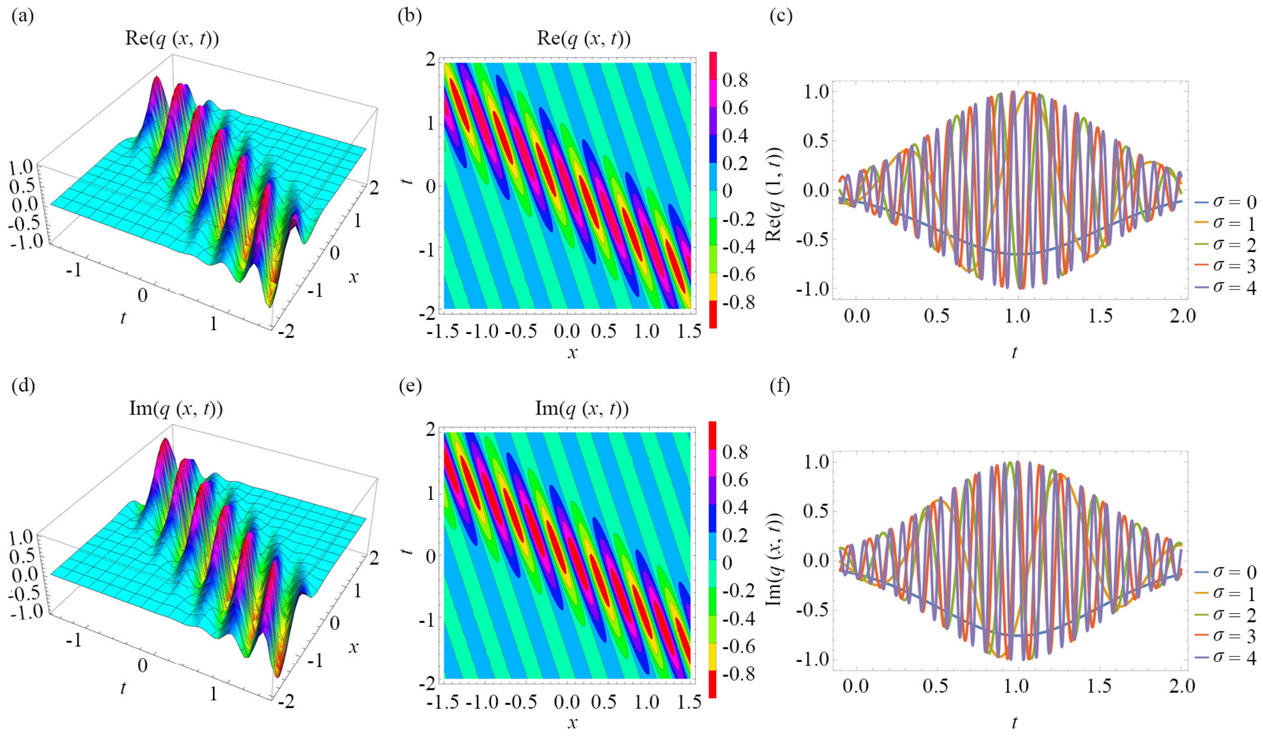

Figure 9. A bright soliton given $\sigma = 4$

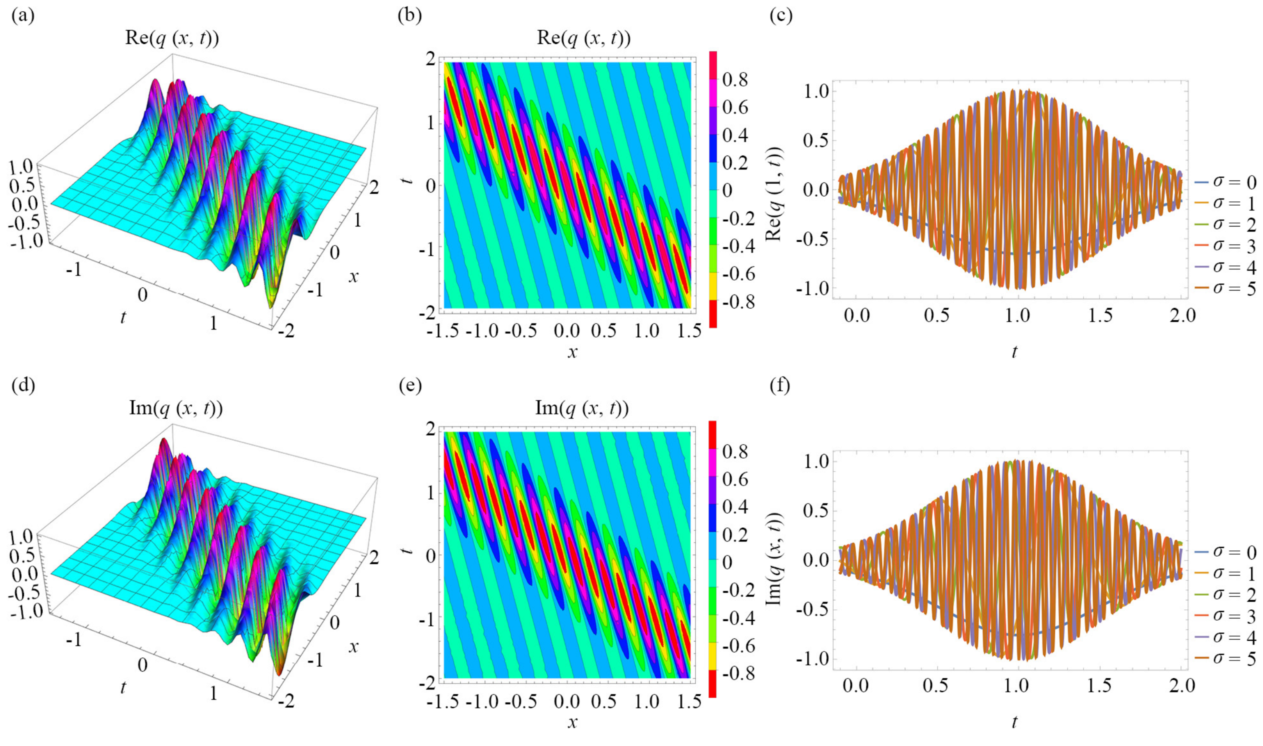

Figure 10. A bright soliton given $\sigma = 5$

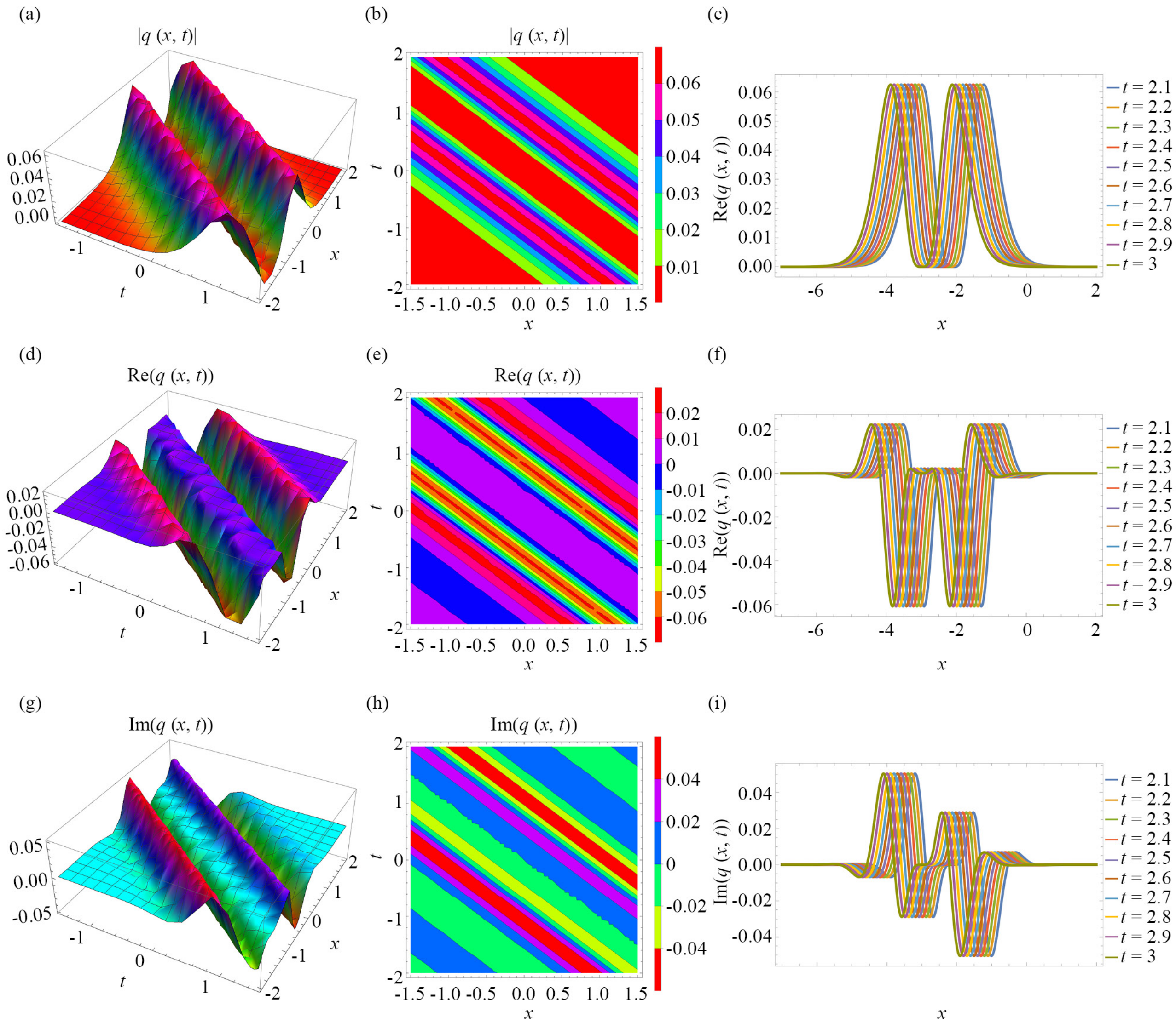

Figure 11. A bright-dark soliton given $\sigma = 0$

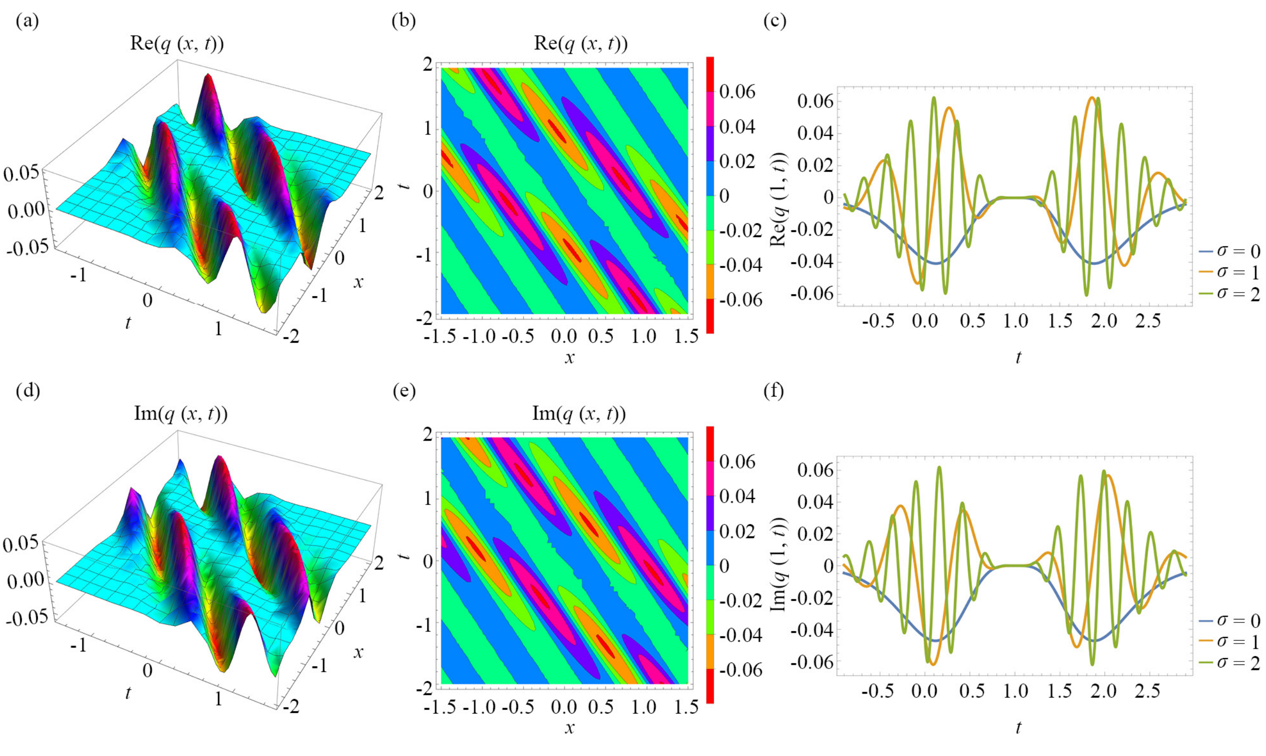

Figure 12. A bright-dark soliton given $\sigma = 2$

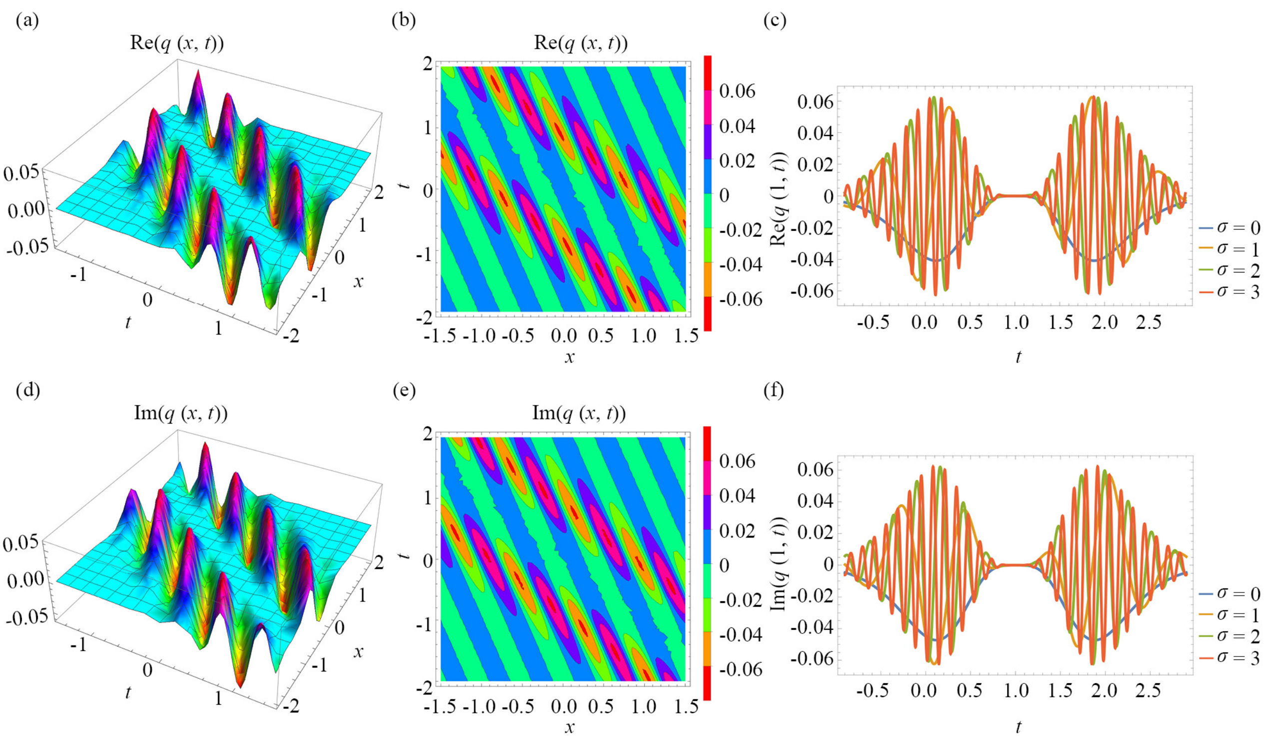

Figure 13. A bright-dark soliton given $\sigma = 3$

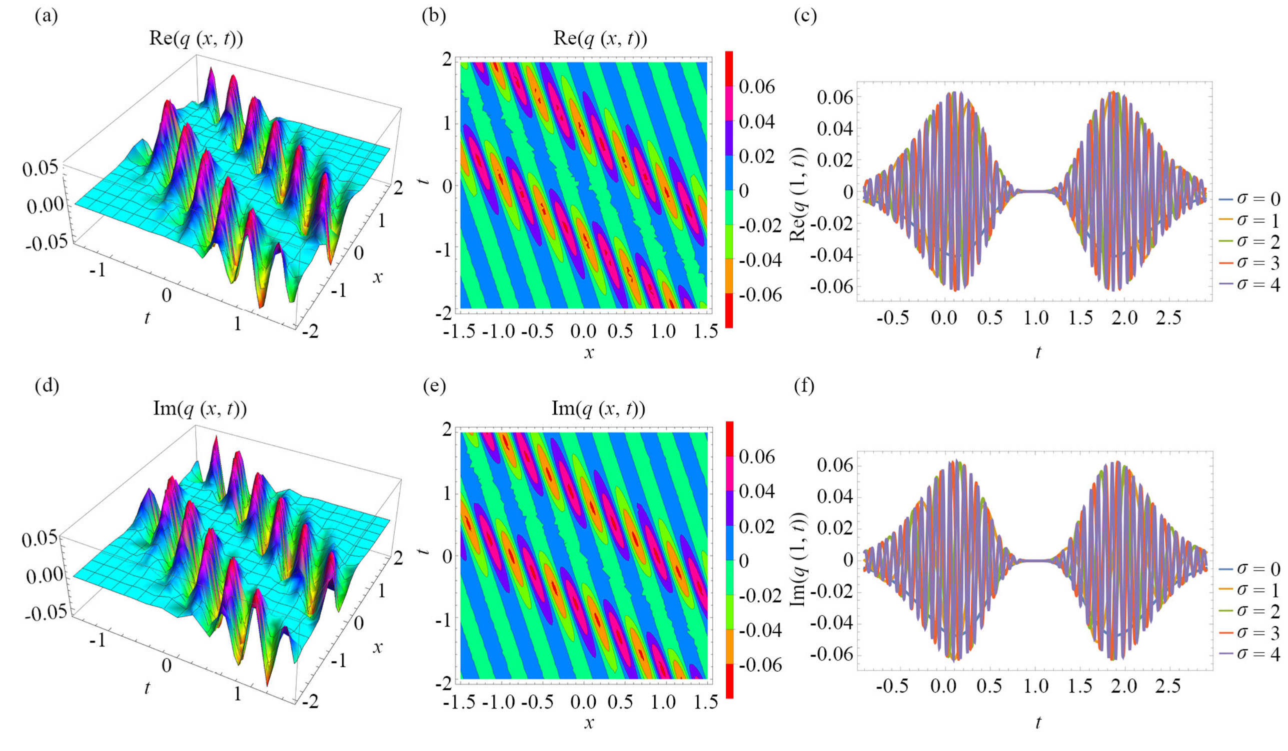

Figure 14. A bright-dark soliton given $\sigma = 4$

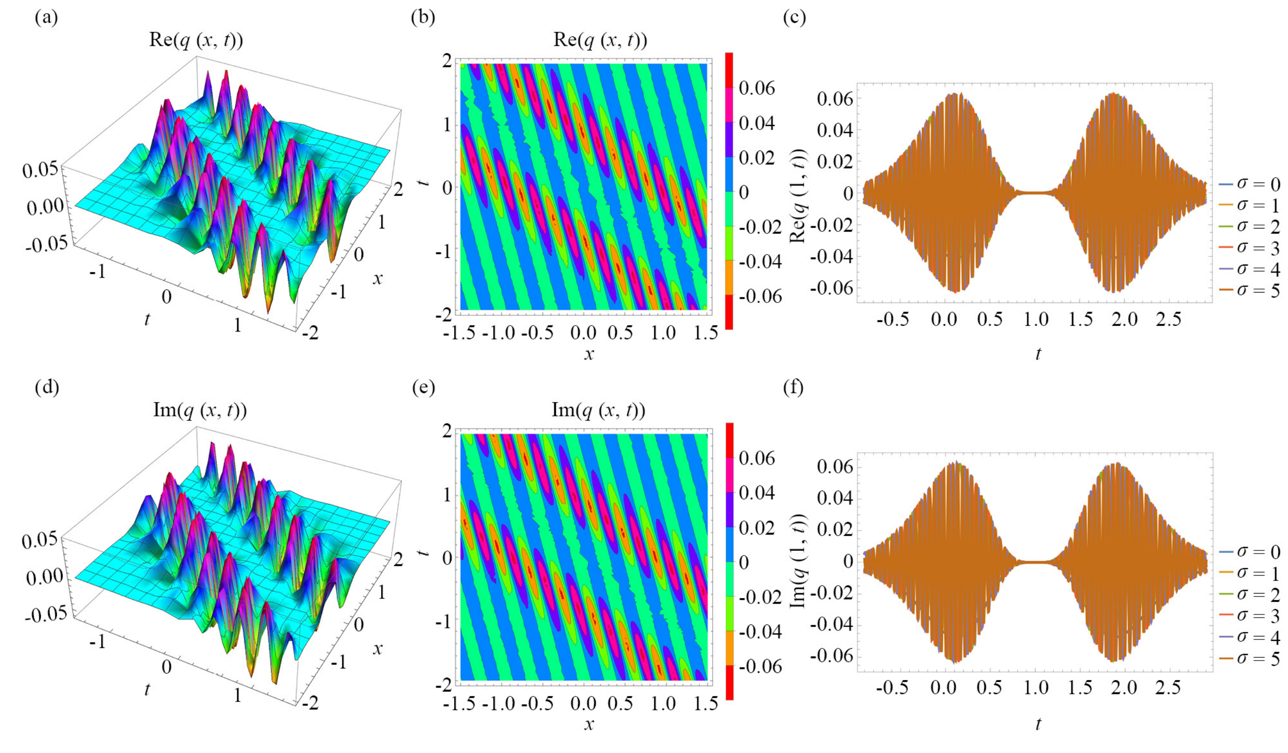

Figure 15. A bright-dark soliton given $\sigma = 5$

5. Conclusions

This study investigates optical solitons governed by the dispersive concatenation model, which captures the interplay of dispersion and nonlinearity in optical fibers. The model incorporates the Kerr nonlinearity and MWN, the latter modeled using Itô calculus to represent real-world fluctuations such as thermal and environmental noise.

To find analytical solutions, the F-expansion method is applied, yielding a variety of soliton structures including bright, dark, singular, and hybrid solitons. The results indicate that MWN primarily affects the soliton phase, leaving the amplitude largely unchanged. This has important implications for phase-sensitive systems in optical communications.

Figures 1-15 illustrate the soliton dynamics under varying noise levels. Dark solitons become shallower and broader, bright solitons experience peak deformation, and hybrid solitons show mixed effects. These visual results support the analytical findings and highlight the destabilizing role of noise.

Compared to previous studies focused on deterministic or noise-free scenarios, this work presents a more realistic perspective by combining nonlinear dispersion and stochastic perturbations. The broader solution set obtained via the F-expansion method offers deeper insights into soliton behavior under noisy conditions. The similarity of our research to the study described in [3] is limited to the common concern for the same model equation. The methods used, however, are significantly different. The study mentioned, identified as [3], uses a sophisticated direct algebraic method, whereas our paper proposes the use of the F-expansion method. These are different and independent methods. In addition, our study offers completely new results that are not considered in the framework of study described in [3]. In addition, the work introduced in reference [3] is solely focused on presenting solutions, including no graphical analysis. In contrast, our paper provides a thorough analysis of the solution results, including the use of graphs. More specifically, we have included graphs that describe the effect of multiplicative white noise on the soliton solution results. These graphically illustrated results are thoroughly investigated in the results and discussion section, in which we highlight the physical importance of all the new solution results.

Future work may extend the model by incorporating power-law SPM or analyzing its behavior in advanced optical media such as dispersion-flattened fibers, birefringent systems, and photonic crystal structures [4–14]. These directions aim to deepen our understanding of soliton robustness in practical settings and broaden the model's applicability to emerging optoelectronic technologies.

Acknowledgement

One of the authors, AB, is grateful to Grambling State University for the financial support he received as the Endowed Chair of Mathematics. This support is sincerely appreciated.

Conflict of interest

The authors declare no competing financial interest.

References

[1] Arnous AH, Biswas A, Yildirim Y, Alshomrani AS. Stochastic perturbation of optical solitons for the concatenation model with power-law of self-phase modulation having multiplicative white noise. *Contemporary Mathematics*. 2024; 5(1): 567-589. Available from: https://doi.org/10.37256/cm.5120244107.

[2] Ekici M, Sarmasik CA. Certain analytical solutions of the concatenation model with a multiplicative white noise in optical fibers. *Nonlinear Dynamics*. 2024; 112(11): 9459-9476. Available from: https://doi.org/10.1007/s11071-024-09478-y.

[3] Arnous AH, Biswas A, Yildirim Y, Alshomrani AS. Optical solitons with dispersive concatenation model having multiplicative white noise by the enhanced direct algebraic method. *Contemporary Mathematics*. 2024; 5(2): 1122-1136. Available from: https://doi.org/10.37256/cm.5220244123.

[4] Ekici M. Stationary optical solitons with complex Ginzburg-Landau equation having nonlinear chromatic dispersion and Kudryashov's refractive index structures. *Physics Letters A*. 2022; 440: 128146. Available from: https://doi.org/10.1016/j.physleta.2022.128146.

[5] Sarmasik CA, Ekici M. Multi wave, kink, breather, Peregrine-like rational and interaction solutions for the concatenation model. *Optical and Quantum Electronics*. 2024; 56(2): 256. Available from: https://doi.org/10.1007/s11082-023-05799-1.

[6] AlQahtani SA, Alngar MEM. Soliton solutions of perturbed NLSE-CQ model in polarization-preserving fibers with cubic-quintic-septic-nonic nonlinearities. *Journal of Optics*. 2024; 53: 3789-3796. To appear. Available from: https://doi.org/10.1007/s12596-023-01526-x.

[7] Arnous AH, Elsherbeny AM, Secer A, Ozisik M, Bayram M, Shah NA, et al. Optical solitons for the dispersive concatenation model with spatio-temporal dispersion having multiplicative white noise. *Results in Physics*. 2024; 56: 107299. Available from: https://doi.org/10.1016/j.rinp.2023.107299.

[8] Jawad AJM, Abu-AlShaeer MJ. Highly dispersive optical solitons with cubic law and cubic-quintic-septic law nonlinearities by two methods. *Al-Rafidain Journal of Engineering Sciences*. 2023; 1(1): 1-8. Available from: https://doi.org/10.61268/sapgh524.

[9] Jihad N, Almuhsan MAA. Evaluation of impairment mitigations for optical fiber communications using dispersion compensation techniques. *Al-Rafidain Journal of Engineering Sciences*. 2023; 1(1): 81-92. Available from: https://doi.org/10.61268/0dat0751.

[10] Wang MY. Optical solitons with perturbed complex Ginzburg-Landau equation in Kerr and cubic-quintic-septic nonlinearity. *Results in Physics*. 2022; 33: 105077. Available from: https://doi.org/10.1016/j.rinp.2021.105077.

[11] Samir I, Badra N, Ahmed HM, Arnous AH. Exploring soliton solutions to sixth order dispersive non-linear Schrödinger equation with Kerr law nonlinearity using modified extended direct algebraic method. *Optical and Quantum Electronics*. 2023; 55(2): 184. Available from: https://doi.org/10.1007/s11082-022-04459-0.

[12] Taema MA, Youssri YH. Third-kind chebyshev spectral collocation method for solving models of two interacting biological species. *Contemporary Mathematics*. 2024; 5(4): 6189-6207. Available from: https://doi.org/10.37256/cm.5420245950.

[13] Youssri YH, Atta AG. Adopted Chebyshev collocation algorithm for modeling human corneal shape via the Caputo fractional derivative. *Contemporary Mathematics*. 2025; 6(1): 1223-1238. Available from: https://doi.org/10.37256/cm.6120256387.

[14] Youssri YH, Alnaser LA, Atta AG. A spectral collocation approach for time-fractional korteweg-de vriesburgers equation via first-kind chebyshev polynomials. *Contemporary Mathematics*. 2025; 6(2): 1501-1519. Available from: https://doi.org/10.37256/cm.6220255948.